THE JOURNAL OF PHYSICAL CHEMISTRY C

Article

pubs.acs.org/JPCC

Unraveling the Influence of Metal Substrates on Graphene Nucleation from First-Principles Study

Lixiang Zhong,[†,‡] Jia Li,[*,†] Yuanchang Li,[*,§] Haizhou Lu,[∥] Hongda Du,[†] Lin Gan,[†] Chengjun Xu,[†] Sum Wai Chiang,[†] and Feiyu Kang[†,‡]

[†]Guangdong Provincial Key Laboratory of Thermal Management Engineering and Materials, Graduate School at Shenzhen, Tsinghua University, Shenzhen 518055, People's Republic of China

[‡]School of Materials Science and Engineering, Tsinghua University, Beijing 100084, People's Republic of China

[§]National Center for Nanoscience and Technology, Beijing 100190, People's Republic of China

[∥]Department of Physics, South University of Science and Technology of China, Shenzhen 518055, People's Republic of China

Supporting Information

ABSTRACT: Using ab initio calculations, we systematically investigate graphene nucleation on 10 representative metal substrates that have been used in graphene growth by chemical vapor deposition. We find that the metal substrates can be divided into three categories with respect to the competition between carbon−carbon (C−C) and carbon−metal (C−M) interactions, which leads to the distinct critical size (N_c) dependence of the smallest graphene precursor on the substrates. The C−M interactions are weak on Ag, Au, Cu, and Co substrates, and the chemical potential of carbon decreases monotonically to approach that of graphene as the size of the carbon clusters increases. We observed an N_c around C_{13}−C_{14} corresponding to the structural transition from a linear chain to sp^2 configuration on these substrates. In contrast, the C−M interactions are strong on Ru, Pt, Rh, and Ir substrates, and the extremely stable carbon monomer thermodynamically determines the larger N_c about C_{19}. The third category is Ni and Pd substrates, for which carbon atoms tend to penetrate into the first layer of the metal substrates, implying a more complicated graphene nucleation mechanism. We also discuss the growth kinetics of the small carbon clusters as well as the effect of the practical environment, like surface defects, on graphene nucleation.

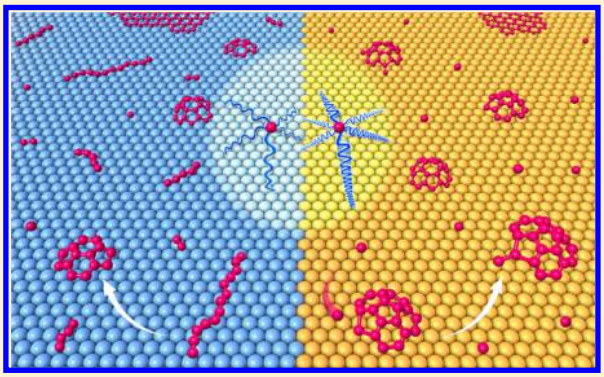

INTRODUCTION

To facilitate the application of graphene, its mass production with high quality and low cost is required. Many methods to synthesize graphene have been reported, including mechanical exfoliation of graphite,[1] thermal decomposition of silicon carbide,[2] reduction of graphene oxides,[3−5] and chemical vapor deposition (CVD) on metal substrates,[6−8] etc. In particular, CVD method shows great promise to produce graphene on a large scale, stimulating extensive activity among physicists, chemists, and material scientists.[9−12] In the CVD process, the nucleation of graphene is important because the density of nucleation is directly related to the quality of graphene. For example, a high density usually leads to graphene with a polycrystalline structure with intrinsic topological defects,[13] which can strongly scatter charge carriers.[14,15] These defects also lower the charge carrier mobility of graphene by about 1 order of magnitude[6,7] as compared to that of graphene obtained by mechanical exfoliation.[16] Therefore, a comprehensive understanding of graphene nucleation on metal substrates, including both energetics and kinetics, is desired to help control the nucleation density and allow growth condition optimization.[17]

To understand graphene nucleation, two issues should be fully addressed. One is the delicate competition between the carbon−carbon (C−C) and carbon−metal (C−M) interactions at the interface between graphene and the metal surface.[18] The other is the property of the smallest stable graphene precursor, including its critical size (N_c) and characteristic configuration. The former intrinsically affects C accumulation, while the latter is closely related to the structure and quality of the ultimate graphene domain as well as growth kinetics. In recent years, considerable effort has been devoted to exploring the structure and energetics of small C clusters on metal surfaces both theoretically and experimentally.[19] Zhang's group[20] first investigated C nucleation in the early stages of graphene growth on Ir (111), Ru (0001), and Cu (111) surfaces, and proposed a novel dimer-based picture instead of the traditional

Received: July 6, 2016
Revised: September 18, 2016
Published: September 21, 2016

DOI: 10.1021/acs.jpcc.6b06750
J. Phys. Chem. C 2016, 120, 23239−23245

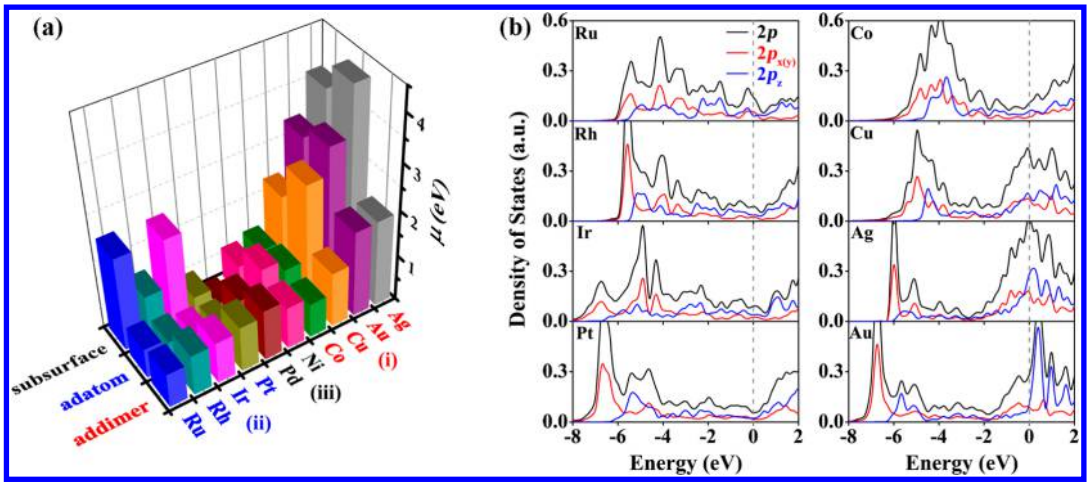

Figure 1. (a) Chemical potentials (μ_N^M) of subsurface C atoms, surface C adatoms, and addimers on different metal substrates. (b) Projected density of states of a C adatom, which has contributions from 2p-electrons, for metal substrates in categories (i) and (ii), corresponding to the ground state for the C adatom. The Fermi level was set to zero.

monomer-based concept. Very recently, they further showed that C−C dimers are the dominant feeding species on Cu substrates using multiscale modeling.[21] Meanwhile, Ding and colleagues[22−24] focused on the structural configuration of small C clusters (C_N, where $N \leq 30$) on four kinds of metal substrates (Rh, Ru, Ni, and Cu). On the basis of extensive calculations of each possible configuration, they originally claimed C_{21}, a fraction of C_{60}, as the unique magic cluster,[23] and 3 years later they found another ultrastable C cluster, C_{24}.[24] In experimental studies, uniform C clusters with a diameter of around 1 nm have been observed by scanning tunneling microscopy (STM) on Ru (0001),[25,26] Rh (111),[27] and Ir (111)[28] surfaces, although their detailed structure and formation process are still unclear. In contrast, the presence of small C clusters on other metal substrates like Cu has not been reported, despite the numerous experimental and theoretical investigations of graphene growth on this metal substrate.

Here, we systematically investigate graphene nucleation on almost all metal substrates that are used in CVD growth of graphene, including Ru, Co, Rh, Ir, Ni, Pd, Pt, Cu, Ag, and Au. In terms of C−C and C−M interactions at these graphene−substrate interfaces, three kinds of nucleation processes are found. Meanwhile, it is also revealed that the graphene precursors all contain pentagons, which offer a continuous driving force for the cluster size to increase. Our findings provide useful insights into the role of metal substrates in graphene nucleation to guide future experimental design. In addition, our study of graphene nucleation on metal substrates is complementary with the study of metallic nanoclusters nucleation on graphene performed by Wang et al.[18]

METHODS

Spin-polarized calculations were performed using density functional theory implemented in the Vienna ab initio simulation package.[29,30] The projected augmented wave potential[31] and generalized gradient approximation with the Perdew−Burke−Ernzerhof functional[32] were used to describe the electron−ion interactions and exchange-correlation energy, respectively. The cutoff energy was set to 400 eV. We used a three-layer slab model to mimic the metal surfaces with the bottom layer fixed at their respective bulk positions. Test calculations using a six-layer model yielded the same results as those using the three-layer model. The separation between two slabs was larger than 15 Å, and the distance between two neighboring C clusters was larger than 12 Å to eliminate spurious interactions. All structures were optimized by the conjugate gradient method until the residual force on each atom was less than 0.01 eV/Å. The climbing image nudged elastic band method[33] and Tersoff−Hamann approximation[34] were used to calculate the energy barriers and simulate STM images, respectively. The structure models and STM images were visualized in the VESTA software.[35] To characterize the stability of C clusters with different numbers of C atoms on metal substrates, we defined the chemical potential of C (μ_N^M) as

$$\mu_N^M = \frac{E - E_0}{N} - \mu_0$$

where E and E_0 are the total energies of metal substrates with and without a C cluster, respectively. N is the number of C atoms, and μ_0 is the energy per atom of graphene. The μ_N^M defined here has also been used previously to study the growth of carbon nanotubes or graphene.[23,36] The higher was the μ_N^M, the less stable was the cluster.

RESULTS AND DISCUSSION

We first investigated the interactions of a C monomer and dimer with 10 kinds of metal surfaces: Ru (0001), Co (0001), Rh (111), Ir (111), Ni (111), Pd (111), Pt (111), Cu (111), Ag (111), and Au (111). The chemical potentials (μ_N^M) of the C monomer and dimer on different metals are shown in Table S1 and further summarized in Figure 1a. It reveals that the 10 metal substrates can be divided into three categories: (i) Au, Ag, Cu, and Co substrates, for which the addimer gives the most favorable energy and the C monomer prefers the subsurface site, (ii) Ru, Rh, Ir, and Pt substrates, which have the smallest μ corresponding to C adatom adsorption on the surface, and (iii) Pd and Ni substrates, for which the C atom located in the subsurface has the smallest μ. These results indicate that the distinct C−C and C−M interactions on different metal substrates affect graphene nucleation. Because a C adatom penetrating the topmost layer of a metal substrate gives the most stable state for Pd and Ni substrates, this

DOI: 10.1021/acs.jpcc.6b06750
J. Phys. Chem. C 2016, 120, 23239−23245

naturally leads to a bulk-mediated growth mode, and graphene would be obtained by precipitation from the bulk metal. It means when the C atom is catalytically decomposed from the gaseous carbon source, it can be easily dissolved into the bulk metal due to the high carbon solubility of such metals. When the amount of the dissolved C reached the limit with the decreasing temperature, the C precursor will precipitate from the bulk metal. As the carbon cluster grows larger, it becomes more favorable as compared to carbon at subsurface sites, and graphene forms eventually.[37,38] The situation is different for metal substrates in categories (i) and (ii), where a surface-mediated nucleation process can be expected. In this work, we focus on graphene nucleation on metal substrates in (i) and (ii).

Comparing μ of the addimer with that of the adatom on different substrates clearly reveals that the C−C interaction is stronger for category (i), while the C−M interaction is stronger for (ii). To better understand this, we plotted the projected density of states (PDOS) of a C atom, which has contributions from 2p-electrons, corresponding to the ground state of the C adatom, on the different substrates, as shown in Figure 1b. An interesting finding is the close relation between μ and the PDOS of a C adatom at the Fermi level; that is, a higher PDOS (especially for the p_z state) generally corresponds to a higher μ, and vice versa. For example, the PDOS of a C adatom on a coinage metal (Cu, Ag, and Au) substrate has a peak at the Fermi level, and μ is >2.5 eV. Conversely, for metal substrates in category (ii), there are no PDOS peaks around the Fermi level, and μ is <0.65 eV. These trends are quite understandable. When the C−M coupling is strong, the originally degenerate 2p states of the C atom will split into bonding and antibonding states, and the PDOS peaks around the Fermi level will disappear. In contrast, when the C−M coupling is weak, the 2p states of the C atom largely remain atomic-like, and the PDOS peaks lie around the Fermi level. In addition, it is worth noting that for category (i) metals, especially for coinage metals, the PDOS peaks around the Fermi level disappeared after adding a C atom to form an addimer as shown in Figure S1. It indicates that two carbon atoms will form a strong covalent bond and weaken the interaction between C atom and metal substrate (can also be seen from Table S2) when combined into a dimer on these substrates.

The competition between C−C and C−M interactions can also be reflected by the bond length of the C−C addimer. A shorter bond length indicates a stronger C−C interaction and in turn a weaker C−M interaction. The calculated bond lengths of a C−C addimer on the different metal surfaces exhibited the sequence of Ag (1.284 Å) < Au (1.297 Å) < Cu (1.302 Å) < Co (1.345 Å) < Ru/Pt (1.373 Å) < Rh (1.387 Å) < Ir (1.400 Å). For metal substrates in category (i) except for Co, the bond length is typically between those of a C≡C triple bond (1.208 Å) and C═C (1.333 Å). For substrates in category (ii), the values are larger than that of a typical C═C bond but smaller than that of a C−C one (1.541 Å). This further confirms that the metal substrates in category (ii) have stronger C−M interactions than C−C ones, consistent with the PDOS analysis.

Because the C monomer and addimer only represent the initial stage of the graphene nucleation process, it is necessary to study larger C clusters to reveal N_c and the configuration of the smallest graphene precursor. Next, we track the energetics of C clusters (≤24) on typical metal surfaces Cu (111), Co (0001), Rh (111), and Ir (111). Only these four surfaces were used because of the huge computational cost of searching for the minimum energy structure of complex systems. Note that Cu and Co belong to category (i), while Rh and Ir belong to category (ii). Such a selection means that we can compare the nucleation not only between different categories, but also within the same category to gain insights into the remaining metal substrates.

The possible structures of C_N were carefully explored; Figure 2 shows their respective μ_N^M corresponding to the ground-state

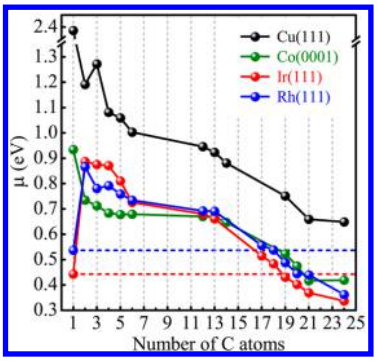

Figure 2. Chemical potentials of the ground-state structures of C clusters on Cu (111), Co (0001), Rh (111), and Ir (111) surfaces. Lines are provided as visual guides. The two horizontal dashed lines represent the chemical potentials of C monomers on Rh (111) and Ir (111) surfaces.

structure as a function of C number N. It is found that μ_N^M decreases monotonically as N increases on Cu (111) and Co (0001) surfaces, with only the exception of C_2 on Cu (111). This indicates the graphene precursor on these metals would spontaneously enlarge without any nucleation barrier as long as the C source is continuously supplied. However, it will be shown below that the smallest size of graphene precursor is still present because of both thermodynamic and kinetic effects. For Rh (111) and Ir (111) surfaces, μ_1^M is lower than that of C_N until it reaches a critical size, that is, C_{19} (Figure 2). In this regard, all C_N between C_1 and C_{19} should be energetically unstable and not exist in reality, thus leading to a distinct nucleation process from Cu (111) and Co (0001) surfaces.

The curves depicted in Figure 2 also provide us with other useful information. For example, C_2 is more stable than its neighboring C_1 and C_3 on a Cu (111) surface, which agrees with the recent claim that C_2 is the dominant feeding species in graphene formation.[21] For the same size C_N ($N \geq 3$), μ^{Cu} is always ~0.30 eV larger than μ^{Co}, μ^{Rh}, and μ^{Ir}, but the latter three only differ slightly. This originates from the different coupling strengths between p−s and p−d orbitals. Note that the other two noble metals Ag and Au also characterized by p−s coupling give even higher μ than μ^{Cu} when $N \leq 2$ (see Figure 1a). From Co to Rh to Ir, which are located in the same column in the periodic table, the atomic radius increases gradually and μ_N^M changes only a little, suggesting a weak dependence of p−d hybridization on 3d, 4d, and 5d electrons. Furthermore, it seems that another universal number (N_t) exists around 13−14. When $N < N_t$, μ_N^M changes slowly, while when $N > N_t$, μ_N^M decreases rapidly. This sharp change may correspond to a structural transition.

Figure 3 plots the representative geometries to determine critical N_c on Co (0001) and Cu (111) surfaces. Moreover, the optimized structures and chemical potentials of C clusters with different numbers of C atoms ($1 \leq N \leq 24$) on Co (0001) and

DOI: 10.1021/acs.jpcc.6b06750
J. Phys. Chem. C 2016, 120, 23239−23245

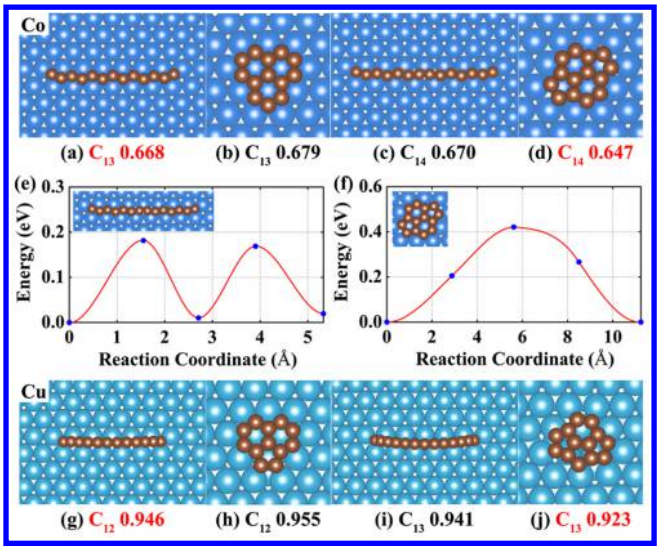

Figure 3. Transitions from C chains to sp^2 compact clusters on (a–d) Co (0001) and (g–j) Cu (111) surfaces, and diffusion barriers of the (e) C chain and (f) sp^2 compact cluster both composed of 14 C atoms on a Co (0001) surface.

Cu (111) surfaces are shown in Figures S2 and S3. For a Co (0001) surface, a C monomer occupying the subsurface six-coordinated site is the most stable, at 0.12 eV lower in energy than adsorption on the surface, while the two C atoms forming an addimer on the surface decrease μ by about 0.077 eV (see Table S1). Further increasing N, the geometries become more complex. By examining the energetics of many possible configurations, we find that the zigzag-type linear carbon chain is always the ground state for small N. For example, when N = 5 and 6, the linear chain configurations are energetically more favorable by 1.37 and 0.85 eV than that of pentagonal and hexagonal configurations, respectively.[39]

However, the zigzag C chains are still far less stable than graphene, and the final products are graphene composed of sp^2-hybridized C atoms. Therefore, there must be a structural transition from zigzag C chains to sp^2 compact C clusters. This structural transition means the thermodynamical competition between C chains and sp^2 compact C clusters configurations. Gao et al.[40] proposed that C_{12} is the critical cluster for the transition on a Ni (111) surface. Herein, we found it occurs at N = 14 in our previous work,[39] also shown in Figure 3a–d; that is, the smallest sp^2 compact cluster more stable than C chains on Co (0001) is the C_{14} composed of two hexagons and two pentagons (Figure 3d), which has μ 0.023 eV lower than that of the corresponding C chain (Figure 3c). The energy difference provides the possibility of the coexistence of the linear and sp^2 configurations when the size of the C cluster is around 13–14. Further increasing N, μ of the sp^2 compact structure decreases, while that of the zigzag chain is largely insensitive to N, as can be seen for the values corresponding to N = 3–13 in Figure 2. Such different trends are easily understood because there is an additional stabilization gain from the formation of conjugated π bonds in the sp^2 compact structure, while each C couples to the metal almost equally in the zigzag chain structure.

Above, we discussed the energetics of C_N on a Co (0001) surface. Another critical factor in determining whether a certain C_N can be the smallest graphene precursor is its kinetic stability. Because the temperature used for graphene growth by CVD is very high, usually around 1000 K, the diffusion should be quite fast even for small C clusters. The effective precursor must be kinetically stable; that is, it has to experience a high enough diffusion barrier so that it can stably locate at the ground-state position to capture mobile C atoms. According to our calculations, the diffusion barrier of a C monomer on a Co (0001) surface is very small (0.27 eV), and those for linear C_{13} or C_{14} chains are less than 0.20 eV. In sharp contrast, the corresponding C_{13} and C_{14} sp^2 compact structures exhibit much higher diffusion barriers of 0.92 and 0.42 eV, respectively. This indicates that the kinetic stabilities of the C_{13} and C_{14} sp^2 compact structures are higher than those of the corresponding chains (see Figure 3e,f). Considering both the thermodynamic and the kinetic factors, the C_{14} cluster composed of two pentagons and two hexagons would serve as the smallest graphene precursor for CVD growth of graphene on a Co (0001) surface.

The situation on a Cu (111) surface is very similar to that on a Co (0001) surface; the C monomer also prefers the subsurface six-coordinated site, and the addimer has a lower μ than that of the monomer by about 0.61 eV. A linear nanoarch configuration is the ground state until N = 13, as shown in Figure 3g–j, consistent with a previous report.[41] Interestingly, the compact C_{13} cluster consists of one hexagon and three pentagons on Cu (111) (Figure 3j) instead of the more symmetric configuration that contains only three hexagons on Co (0001) (Figure 3b). Likewise, the sp^2 compact C_{13} and C_{14} also have relatively larger diffusion barriers of 0.75 and 0.78 eV, respectively, as compared to those of the nanoarches.

From what has been discussed above, we know that a critical N_c exists corresponding to the structural transition from linear to sp^2 compact configuration on Co (0001) and Cu (111) surfaces. Importantly, the transition substantially enhances the kinetic stability of the C cluster. Moreover, the sp^2 C clusters, for example, C_{14}, C_{19}, C_{21}, and C_{24} (see Figures S2 and S3), always possess at least one pentagon even if it lowers the symmetry, implying that pentagons play an important role in stabilizing C clusters. Such a pentagon-containing preference can decrease the number of edge atoms, which consequently lowers the edge formation energy.[40] Besides, the barrier of annealing the edge pentagon into a hexagon on Cu (111) is 1.39 eV, which ensures the continuous growth of graphene at the typical growth temperature. Given the high consistency between Co and Cu substrates, we predict that these should be general phenomena for other metal substrates in category (i) like Au and Ag.

We now turn to the cases of Rh (111) and Ir (111) surfaces that represent the metal substrates category (ii). Figure S4 shows the optimized structures and chemical potentials of C clusters with different numbers of C atoms ($1 \le N \le 24$) on Rh (111) and Ir (111) surfaces. Unlike in category (i), C monomer adsorption on these metal surfaces is extremely stable because the μ of addimer increases largely, as shown in Figure 2. In consideration of the formation of the large C cluster (C_{19}), despite the high stability of monomer, the increased chemical potential of C atoms with the increasing concentration of C provides the driving force for the aggregation of C monomers. Also, kinetically, the diffusion barriers of C monomer on Rh (111) and Ir (111) are 0.75 and 0.76 eV, respectively, which allows the fast diffusion of C monomers on these substrates at the experimental growth temperature. Akin to the Co and Cu substrates, a structural transition from chain to sp^2 compact is observed, which occurs around C_{12}–C_{14} on the Rh and Ir

DOI: 10.1021/acs.jpcc.6b06750
J. Phys. Chem. C 2016, 120, 23239–23245

substrates. Nevertheless, it is only from C_{19} that μ becomes lower than that of the carbon monomer, giving rise to a thermodynamically determined N_c of the graphene precursor on the Rh and Ir substrates. We also calculated the diffusion barriers of C_{19} on Rh (111) and Ir (111) surfaces. As expected, the barriers on Rh and Ir surfaces are as high as 1.83 and 2.94 eV, respectively, because of the relatively large size of the C cluster and strong C−M interaction. Such high diffusion barriers naturally hamper the movement of C clusters as well as their agglomeration.

In detail, C_{19} is composed of a central pentagon surrounded by another pentagon and four hexagons, as shown in the top inset of Figure 4a. Surprisingly, C_{19} has two adjacent pentagons.

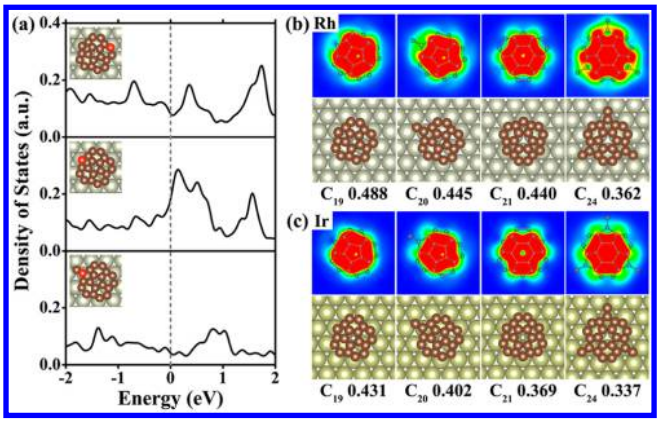

Figure 4. (a) Projected density of states of different edge C in C_{19} on Rh (111) and the stabilized edge C in C_{20}. Simulated scanning tunneling microscopy images and atomic structures of C clusters more stable than a C adatom on (b) Rh (111) and (c) Ir (111).

Pentagons exist in many C clusters like fullerene, but they must be isolated[42] to lower the system energy because they induce local curvature. However, here the large curvature can help the central part of the C cluster to lift off the metal substrate and ultimately develop as graphene. With two more C atoms, C_{21}, the cluster behaves as a fraction of fullerene containing three isolated pentagons connected by four hexagons with C_{3v} symmetry.[23]

To fully understand the role of pentagons in graphene growth, we calculated the PDOS corresponding to the different C edge atoms on Rh (111), as illustrated in Figure 4a. Generally, the sp^2 carbon is inert, so we focused on the C atoms with only two neighboring C atoms. The C atoms belonging to the hexagon have a small PDOS population at the Fermi level (top of Figure 4a), while that for the pentagon contains a peak (middle of Figure 4a). This indicates the distinct chemical activity of the hexagon and pentagon, and that a new C atom naturally attaches to the edge C atom of a pentagon. After this, the edge C atom of the pentagon becomes sp^2 coordinated, the peak near the Fermi level disappears, and consequently the edge C atom becomes chemically inert (bottom of Figure 4a). It is noted that a similar pentagon-containing phenomenon is also observed on the metal substrates in category (i).

The simulated STM images of C_{19} and some other typical C clusters that are more stable than a C adatom on Rh (111) and Ir (111) surfaces are shown in Figure 4b and c, respectively. It is noteworthy that C clusters with a diameter of around 1 nm have been observed experimentally on Ru (0001),[25,26] Rh (111),[27] and Ir (111)[28] surfaces. The C clusters with high symmetry of C_{3v} detected on Rh (111)[27] and Ru (0001)[25] surfaces are believed to be C_{21} or C_{24} clusters.[23,24] However, the STM images reveal that C clusters with a diameter of around 1 nm without C_{3v} symmetry also exist on Rh (111)[27] and Ru (0001)[25,26] surfaces, as well as on Ir (111)[28] surfaces. By comparing our simulated STM images with these experimental results, we believe that these low-symmetry C clusters with a diameter of around 1 nm are C_{19} or C_{20} clusters. In contrast, there is no experimental evidence for the existence of a kinetic C_N around C_{13}−C_{14} on any metal substrate. Figure 2 indicated that once these clusters form, μ^{TM} decreases rapidly, implying fast growth. Therefore, their rather small size and short lifetime make it difficult to observe such kinetically determined N_c. More simulated STM images of these critical C clusters are presented in Figure S5.

From our simulations, we can construct a picture of graphene growth on metal substrates. During the initial stage, the fast-moving C atoms aggregate together occasionally and form C clusters of different sizes. Among them, only those beyond N_c can survive and serve as a graphene nucleus. As a nucleus grows, the edge C atom with the dangling bond behaves as the acceptor site for the clusters with an open configuration, while the pentagon offers the driving force for clusters with a closed configuration. The curvature induced by the pentagons will lift the central part of these C clusters off the metal substrate. Meanwhile, the pentagons continue to move toward the edge of the cluster to keep capturing more mobile C atoms. As the C cluster becomes larger, more hexagons become suspended and ultimately graphene forms.

In reality, metal surfaces possess defects like vacancies and steps that can strongly affect graphene nucleation. However, the effect of defects on graphene nucleation should be distinct for metal substrates in categories (i) and (ii) because of their remarkable difference of N_c. A point defect helps to immobilize C atoms, which makes it easier to reach N_c for the structural transition on metal substrates in category (i). This effect should be weaker for substrates in category (ii) because of their notably large N_c and strong initial C−M coupling. In contrast, a line defect such as a step or dislocation is expected to strongly affect graphene nucleation on metal substrates in category (ii) because of its ability to simultaneously trap enough carbon atoms for nucleation. The tendency of graphene nucleation to occur at steps has been observed on all of the metal substrates in category (ii), that is, Ru,[43] Rh,[27] Ir,[28] and Pt[44] surfaces. In addition, as the temperature of CVD-growth graphene can be as high as ∼1000 K, the effect of vibrational entropy should be taken into account. The vibrational entropy is mainly related to the structure of carbon clusters. Generally, the sp^2 cluster usually has a smaller entropy than the carbon chain with the same cluster size. Taking an example of Cu(111) surface, we calculate the vibrational entropies of carbon chains and sp^2 clusters around C_{13} at 1000 K. As shown in Table S3, the vibrational entropy lowers the chemical potentials of carbon chains by 0.4 eV, while it is only 0.3 eV for sp^2 clusters. The vibrational entropy then has a larger effect on carbon chains than on sp^2 clusters, demanding a larger critical nucleation size N_c to offset the effect of entropy.

CONCLUSIONS

Three kinds of nucleation were found for CVD growth of graphene on different metal substrates. The coinage metal and Co substrates have a kinetic smallest graphene precursor around C_{13}−C_{14}, corresponding to the structural transition from a linear chain to sp^2 compact cluster. In contrast, the Ru,

DOI: 10.1021/acs.jpcc.6b06750
J. Phys. Chem. C 2016, 120, 23239−23245

Rh, Ir, and Pt substrates have an energetically determined smallest graphene precursor of C_{19}. For Ni and Pd substrates, the C atoms tend to dissolve in the metals, resulting in a distinctly different nucleation mechanism. The different influences of metal substrates on graphene nucleation are associated with their varying characteristics regarding the competition between C−M and C−C coupling. The formation of pentagons is crucial for the decoupling of carbon clusters from the metal surfaces as well as for the enlargement of the graphene precursors.

■ ASSOCIATED CONTENT

Supporting Information

The Supporting Information is available free of charge on the ACS Publications website at DOI: 10.1021/acs.jpcc.6b06750.

Three tables and five figures, showing chemical potentials of carbon monomer and addimer, projected density of states of C addimers, distance between C and metal substrates, carbon clusters on Co (0001) surface, carbon clusters on Cu (111), carbon clusters on Rh (111) and Ir (111), simulated STM images of some typical clusters on metal surfaces, and effect of entropy on graphene nucleation at high temperature (PDF)

■ AUTHOR INFORMATION

Corresponding Authors

*Phone: +86-755-26033022. E-mail: lijia@phys.tsinghua.edu.cn.

*Phone: +86-10-82545624. E-mail: liyc@nanoctr.cn.

Notes

The authors declare no competing financial interest.

■ ACKNOWLEDGMENTS

This work was supported by the Ministry of Science and Technology of China (Grant no. 2014CB932400), the National Natural Science Foundation of China (Grant nos. 11304053, 11104155, and 51232005), Shenzhen Projects for Basic Research (Grant nos. JCYJ20120831165730910 and KQCX20140521161756227), and the Guangdong Province Innovation R&D Team Plan for Energy and Environmental Materials (Grant Nno. 2009010025). We thank Prof. Zhongfan Liu from Peking University for many helpful discussions. Tianjin Supercomputing Center is also acknowledged for allowing the use of computational resources including TIANHE-1.

■ REFERENCES

(1) Novoselov, K. S.; Geim, A. K.; Morozov, S. V.; Jiang, D.; Zhang, Y.; Dubonos, S. V.; Grigorieva, I. V.; Firsov, A. A. Electric Field Effect in Atomically Thin Carbon Films. *Science* **2004**, *306*, 666−669.

(2) Berger, C.; et al. Electronic Confinement and Coherence in Patterned Epitaxial Graphene. *Science* **2006**, *312*, 1191−1196.

(3) Stankovich, S.; Dikin, D. A.; Dommett, G. H.; Kohlhaas, K. M.; Zimney, E. J.; Stach, E. A.; Piner, R. D.; Nguyen, S. T.; Ruoff, R. S. Graphene-Based Composite Materials. *Nature* **2006**, *442*, 282−286.

(4) Chen, W. F.; Yan, L. F.; Bangal, P. R. Chemical Reduction of Graphene Oxide to Graphene by Sulfur-Containing Compounds. *J. Phys. Chem. C* **2010**, *114*, 19885−19890.

(5) Chen, D.; Feng, H.; Li, J. Graphene Oxide: Preparation, Functionalization, and Electrochemical Applications. *Chem. Rev.* **2012**, *112*, 6027−6053.

(6) Li, X.; et al. Large-Area Synthesis of High-Quality and Uniform Graphene Films on Copper Foils. *Science* **2009**, *324*, 1312−1314.

(7) Reina, A.; Jia, X.; Ho, J.; Nezich, D.; Son, H.; Bulovic, V.; Dresselhaus, M. S.; Kong, J. Large Area, Few-Layer Graphene Films on Arbitrary Substrates by Chemical Vapor Deposition. *Nano Lett.* **2009**, *9*, 30−35.

(8) Zhang, Y.; Zhang, L.; Zhou, C. Review of Chemical Vapor Deposition of Graphene and Related Applications. *Acc. Chem. Res.* **2013**, *46*, 2329−2339.

(9) Pletikosic, I.; Kralj, M.; Pervan, P.; Brako, R.; Coraux, J.; N'Diaye A, T.; Busse, C.; Michely, T. Dirac Cones and Minigaps for Graphene on Ir(111). *Phys. Rev. Lett.* **2009**, *102*, 056808.

(10) Li, X.; Magnuson, C. W.; Venugopal, A.; Tromp, R. M.; Hannon, J. B.; Vogel, E. M.; Colombo, L.; Ruoff, R. S. Large-Area Graphene Single Crystals Grown by Low-Pressure Chemical Vapor Deposition of Methane on Copper. *J. Am. Chem. Soc.* **2011**, *133*, 2816−2819.

(11) Zhang, W. H.; Wu, P.; Li, Z. Y.; Yang, J. L. First-Principles Thermodynamics of Graphene Growth on Cu Surfaces. *J. Phys. Chem. C* **2011**, *115*, 17782−17787.

(12) Sutter, P. W.; Flege, J. I.; Sutter, E. A. Epitaxial Graphene on Ruthenium. *Nat. Mater.* **2008**, *7*, 406−411.

(13) Zhang, J.; Zhao, J.; Lu, J. Intrinsic Strength and Failure Behaviors of Graphene Grain Boundaries. *ACS Nano* **2012**, *6*, 2704−2711.

(14) Yazyev, O. V.; Louie, S. G. Electronic Transport in Polycrystalline Graphene. *Nat. Mater.* **2010**, *9*, 806−809.

(15) Zhang, Z.; Yang, Y.; Xu, F.; Wang, L.; Yakobson, B. I. Unraveling the Sinuous Grain Boundaries in Graphene. *Adv. Funct. Mater.* **2015**, *25*, 367−373.

(16) Bolotin, K. I.; Sikes, K. J.; Jiang, Z.; Klima, M.; Fudenberg, G.; Hone, J.; Kim, P.; Stormer, H. L. Ultrahigh Electron Mobility in Suspended Graphene. *Solid State Commun.* **2008**, *146*, 351−355.

(17) Zhang, X.; Li, H.; Ding, F. Self-Assembly of Carbon Atoms on Transition Metal Surfaces–Chemical Vapor Deposition Growth Mechanism of Graphene. *Adv. Mater.* **2014**, *26*, 5488−5495.

(18) Wang, B.; Bocquet, M. L. Monolayer Graphene and H-Bn on Metal Substrates as Versatile Templates for Metallic Nanoclusters. *J. Phys. Chem. Lett.* **2011**, *2*, 2341−2345.

(19) Wu, P.; Zhang, W.; Li, Z.; Yang, J. Mechanisms of Graphene Growth on Metal Surfaces: Theoretical Perspectives. *Small* **2014**, *10*, 2136−2150.

(20) Chen, H.; Zhu, W.; Zhang, Z. Contrasting Behavior of Carbon Nucleation in the Initial Stages of Graphene Epitaxial Growth on Stepped Metal Surfaces. *Phys. Rev. Lett.* **2010**, *104*, 186101.

(21) Wu, P.; Zhang, Y.; Cui, P.; Li, Z.; Yang, J.; Zhang, Z. Carbon Dimers as the Dominant Feeding Species in Epitaxial Growth and Morphological Phase Transition of Graphene on Different Cu Substrates. *Phys. Rev. Lett.* **2015**, *114*, 216102.

(22) Gao, J.; Yip, J.; Zhao, J.; Yakobson, B. I.; Ding, F. Graphene Nucleation on Transition Metal Surface: Structure Transformation and Role of the Metal Step Edge. *J. Am. Chem. Soc.* **2011**, *133*, 5009−5015.

(23) Yuan, Q.; Gao, J.; Shu, H.; Zhao, J.; Chen, X.; Ding, F. Magic Carbon Clusters in the Chemical Vapor Deposition Growth of Graphene. *J. Am. Chem. Soc.* **2012**, *134*, 2970−2975.

(24) Gao, J.; Ding, F. The Structure and Stability of Magic Carbon Clusters Observed in Graphene Chemical Vapor Deposition Growth on Ru(0001) and Rh(111) Surfaces. *Angew. Chem., Int. Ed.* **2014**, *53*, 14031−14035.

(25) Cui, Y.; Fu, Q.; Zhang, H.; Bao, X. Formation of Identical-Size Graphene Nanoclusters on Ru(0001). *Chem. Commun.* **2011**, *47*, 1470−1472.

(26) Lu, J.; Yeo, P. S.; Gan, C. K.; Wu, P.; Loh, K. P. Transforming C60 Molecules into Graphene Quantum Dots. *Nat. Nanotechnol.* **2011**, *6*, 247−252.

(27) Wang, B.; Ma, X.; Caffio, M.; Schaub, R.; Li, W. X. Size-Selective Carbon Nanoclusters as Precursors to the Growth of Epitaxial Graphene. *Nano Lett.* **2011**, *11*, 424−430.

(28) Coraux, J.; T N'Diaye, A.; Engler, M.; Busse, C.; Wall, D.; Buckanie, N.; Meyer zu Heringdorf, F. J.; van Gastel, R.; Poelsema, B.;

DOI: 10.1021/acs.jpcc.6b06750
J. Phys. Chem. C 2016, 120, 23239−23245

Michely, T. Growth of Graphene on Ir(111). *New J. Phys.* **2009**, *11*, 023006.
(29) Kresse, G.; Furthmüller, J. Efficiency of Ab-Initio Total Energy Calculations for Metals and Semiconductors Using a Plane-Wave Basis Set. *Comput. Mater. Sci.* **1996**, *6*, 15−50.
(30) Kresse, G.; Furthmüller, J. Efficient Iterative Schemes Forab Initiototal-Energy Calculations Using a Plane-Wave Basis Set. *Phys. Rev. B: Condens. Matter Mater. Phys.* **1996**, *54*, 11169−11186.
(31) Blochl, P. E. Projector Augmented-Wave Method. *Phys. Rev. B: Condens. Matter Mater. Phys.* **1994**, *50*, 17953−17979.
(32) Perdew, J. P.; Burke, K.; Ernzerhof, M. Generalized Gradient Approximation Made Simple. *Phys. Rev. Lett.* **1996**, *77*, 3865−3868.
(33) Henkelman, G.; Uberuaga, B. P.; Jonsson, H. A Climbing Image Nudged Elastic Band Method for Finding Saddle Points and Minimum Energy Paths. *J. Chem. Phys.* **2000**, *113*, 9901−9904.
(34) Tersoff, J.; Hamann, D. R. Theory and Application for the Scanning Tunneling Microscope. *Phys. Rev. Lett.* **1983**, *50*, 1998−2001.
(35) Momma, K.; Izumi, F. Vesta 3 for Three-Dimensional Visualization of Crystal, Volumetric and Morphology Data. *J. Appl. Crystallogr.* **2011**, *44*, 1272−1276.
(36) Yazyev, O. V.; Pasquarello, A. Effect of Metal Elements in Catalytic Growth of Carbon Nanotubes. *Phys. Rev. Lett.* **2008**, *100*, 156102.
(37) Kwon, S. Y.; Ciobanu, C. V.; Petrova, V.; Shenoy, V. B.; Bareno, J.; Gambin, V.; Petrov, I.; Kodambaka, S. Growth of Semiconducting Graphene on Palladium. *Nano Lett.* **2009**, *9*, 3985−3990.
(38) Li, X.; Cai, W.; Colombo, L.; Ruoff, R. S. Evolution of Graphene Growth on Ni and Cu by Carbon Isotope Labeling. *Nano Lett.* **2009**, *9*, 4268−4272.
(39) Zhong, L. X.; Li, J.; Du, H. D.; Gan, L.; Kang, F. Y. First Principles Study of Graphene Nucleation on Co(0001) Surface. *New Carbon Mater.* **2016**, in press.
(40) Gao, J.; Yuan, Q.; Hu, H.; Zhao, J.; Ding, F. Formation of Carbon Clusters in the Initial Stage of Chemical Vapor Deposition Graphene Growth on Ni(111) Surface. *J. Phys. Chem. C* **2011**, *115*, 17695−17703.
(41) Van Wesep, R. G.; Chen, H.; Zhu, W.; Zhang, Z. Communication: Stable Carbon Nanoarches in the Initial Stages of Epitaxial Growth of Graphene on Cu(111). *J. Chem. Phys.* **2011**, *134*, 171105.
(42) Kroto, H. W. The Stability of the Fullerenes Cn, with N = 24, 28, 32, 36, 50, 60 and 70. *Nature* **1987**, *329*, 529−531.
(43) Loginova, E.; Bartelt, N. C.; Feibelman, P. J.; McCarty, K. F. Evidence for Graphene Growth by C Cluster Attachment. *New J. Phys.* **2008**, *10*, 093026.
(44) Peng, Z.; Somodi, F.; Helveg, S.; Kisielowski, C.; Specht, P.; Bell, A. T. High-Resolution in Situ and Ex Situ Tem Studies on Graphene Formation and Growth on Pt Nanoparticles. *J. Catal.* **2012**, *286*, 22−29.

DOI: 10.1021/acs.jpcc.6b06750
J. Phys. Chem. C 2016, 120, 23239−23245